Bioconjugate Chemistry

Article

pubs.acs.org/bc

Radiogallium Complex-Conjugated Bifunctional Peptides for Detecting Primary Cancer and Bone Metastases Simultaneously

Kazuma Ogawa,*[,†,‡] Jing Yu,[†] Atsushi Ishizaki,[†] Masaru Yokokawa,[†] Masanori Kitamura,[†] Yoji Kitamura,[§] Kazuhiro Shiba,[§] and Akira Odani[†]

[†]Graduate School of Medical Sciences, Kanazawa University, Kanazawa 920-1192, Japan

[‡]Institute for Frontier Science Initiative, Kanazawa University, Kanazawa 920-1192, Japan

[§]Advanced Science Research Center, Kanazawa University, Kanazawa 920-8640, Japan

ABSTRACT: ^{68}Ga ($T_{1/2}$ = 68 min, a generator-produced nuclide) is an interesting radionuclide for clinical positron emission tomography (PET). Recently, it was reported that radiogallium-labeled 1,4,7,10-tetraazacyclododecane-1,4,7,10-tetraacetic acid (DOTA)-conjugated $(Asp)_n$ peptide [Ga-DOTA-$(Asp)_n$] has great potential for bone metastases imaging. In the current study, a compound containing an aspartic acid peptide linker (D_{11}) as a carrier to bone metastases, an RGD peptide [c(RGDfK) peptide] as a carrier to the primary cancer, and Ga-DOTA as a stable radiometal complex for imaging in one molecule, Ga-DOTA-D_{11}-c(RGDfK), was designed, prepared, and evaluated to detect both the primary cancer and bone metastases simultaneously using ^{67}Ga, which is easy to handle. After DOTA-D_{11}-c(RGDfK) was synthesized using Fmoc-based solid-phase methodology, ^{67}Ga-DOTA-D_{11}-c(RGDfK) was prepared by complexing DOTA-D_{11}-c(RGDfK) with ^{67}Ga. Hydroxyapatite binding assays, integrin binding assays, biodistribution experiments, and single photon emission tomography (SPECT) imaging using tumor-bearing mice were performed using ^{67}Ga-DOTA-D_{11}-c(RGDfK). ^{67}Ga-DOTA-D_{11}-c(RGDfK) was prepared with a radiochemical purity of >97%. *In vitro*, ^{67}Ga-DOTA-D_{11}-c(RGDfK) had a high affinity for hydroxyapatite and $\alpha_v\beta_3$ integrin. *In vivo*, ^{67}Ga-DOTA-D_{11}-c(RGDfK) exhibited high uptake in bone and tumor. The accumulation of ^{67}Ga-DOTA-D_{11}-c(RGDfK) in tumor decreased when it was co-injected with c(RGDfK) peptide. ^{68}Ga-DOTA-D_{11}-c(RGDfK) has great potential as a PET tracer for the diagnosis of both the primary cancer and bone metastases simultaneously.

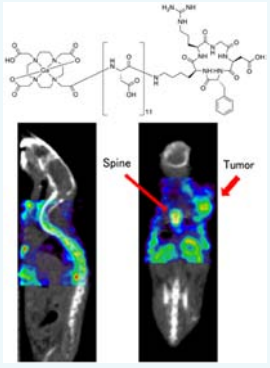

INTRODUCTION

The bone is a suitable environment for tumor to metastasize and grow because it contains abundant proliferation factors; therefore, many kinds of malignant tumors frequently metastasize to the bone.[1,2] With the advances made in treatments for bone metastases, the early detection of bone metastases has become increasingly important. Although progress has been made in anatomical imaging modalities, such as X-ray computed tomography (CT) and magnetic resonance imaging (MRI), over the past few decades, bone scintigraphy in nuclear medicine is the optimum method for detecting bone metastases because of its high sensitivity. Examples include bone-seeking diagnostic radiopharmaceuticals, such as technetium-bisphosphonate complexes [^{99m}Tc-methylenediphosphonate (^{99m}Tc-MDP) and ^{99m}Tc-hydroxymethylenediphosphonate (^{99m}Tc-HMDP)] for single photon emission computed tomography (SPECT) and [^{18}F]NaF for positron emission tomography (PET), which usually localize in metastatic lesions before the appearance of symptoms and radiographic changes.[3] These techniques allow the whole body to be evaluated easily.

Recently, ^{68}Ga has attracted much attention in nuclear medicine as a promising positron-emitting radionuclide because of its radiophysical properties ($T_{1/2}$ = 68 min).[4] ^{68}Ga is a generator-produced nuclide that can be eluted at any time on demand from an in-house generator; it does not require a cyclotron on site. Moreover, unlike ^{99}Mo/^{99m}Tc, which must be purchased frequently because of the short half-life of ^{99}Mo ($T_{1/2}$ = 66 h), the long half-life of the parent nuclide ^{68}Ge ($T_{1/2}$ = 271 d) gives it a long lifespan. Therefore, the generation of bone imaging agents using ^{68}Ga is desirable. Some ^{68}Ga-labeled bone-seeking compounds using bisphosphonate as a carrier to bone, which consist of Ga complex-conjugated bisphosphonate compounds, have been developed.[5−7] In 2013, we reported that Ga-complex conjugated aspartic acid peptides exhibited high accumulation in bone and preferable biodistribution for bone imaging.[8] Therefore, aspartic acid peptides could also function as carriers to bone.

Some pathological processes, such as tumor development, are related to angiogenesis. Integrins are heterodimeric transmembrane glycoproteins that play roles in cell adhesion. Previous studies reported that $\alpha_v\beta_3$ integrin was a marker of angiogenic blood vessels and regulated angiogenesis.[9−11] Moreover, $\alpha_v\beta_3$ integrin is expressed highly on endothelial cells during neovascularization in many kinds of cancers, such as melanoma, glioblastoma, ovarian cancer, and breast cancer, but it is expressed only at very low levels on quiescent endothelial cells.[12] Therefore, $\alpha_v\beta_3$ integrin has garnered much

Received: April 8, 2015
Revised: June 10, 2015
Published: June 18, 2015

DOI: 10.1021/acs.bioconjchem.5b00186
Bioconjugate Chem. 2015, 26, 1561−1570

Scheme 1. Syntheses of Ga-DOTA-D$_n$-c(RGDfK) (n = 0, 8, or 11)[a]

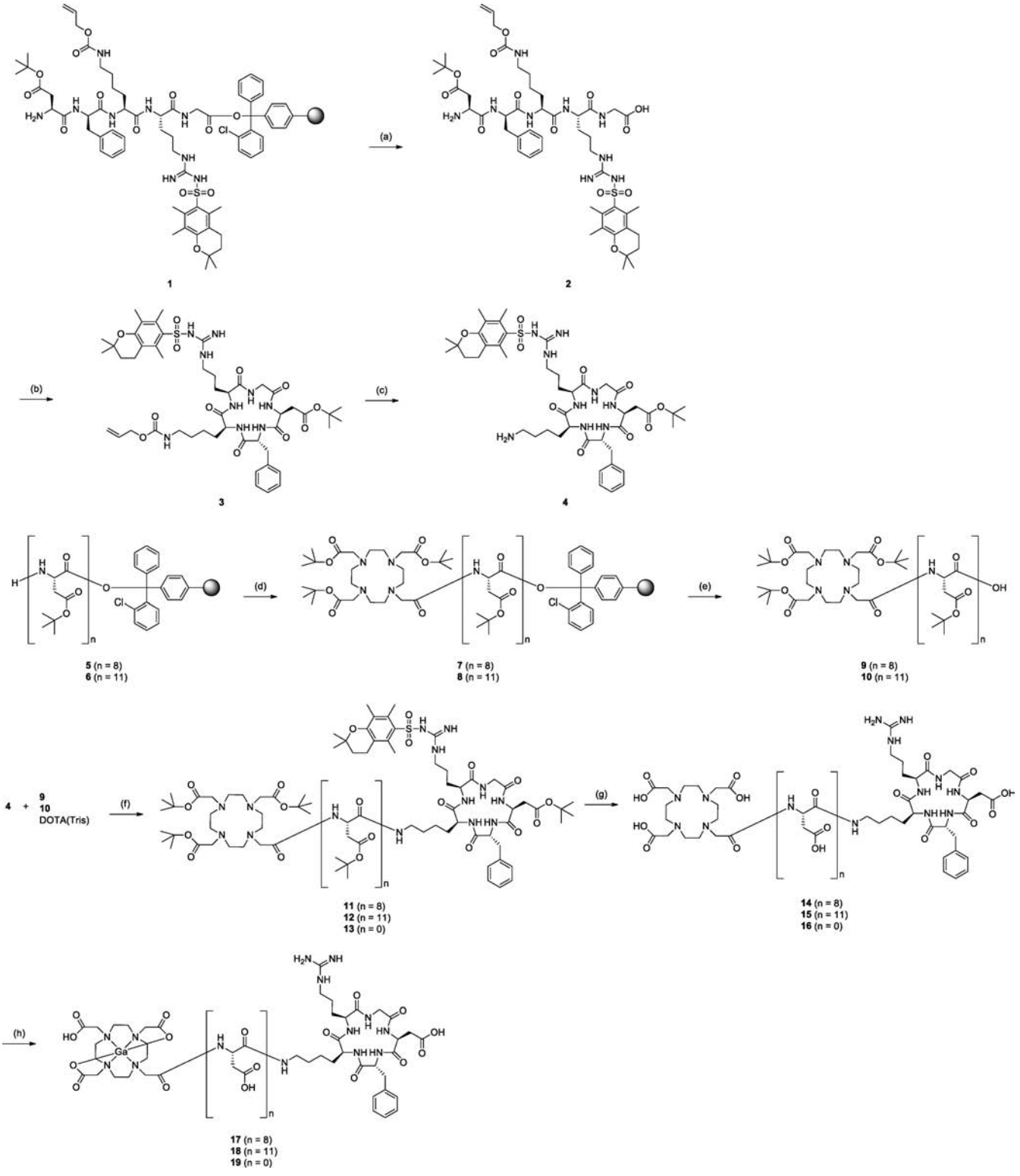

[a]Reagents and conditions: (a) 30% HFIP; (b) diphenylphosphoryl azide, $NaHCO_3$; (c) $Pd(PPh_3)_4$/acetic acid/*N*-methylmorpholine (37:2:1); (d) 1,4,7,10-tetraazacyclododecane-1,4,7-tris(t-butyl acetate), HOBt, DIPCI; (e) 30% HFIP; (f) HOBt, DIPCI; (g) 95% TFA, 2.5% triisopropylsilane, 2.5% H_2O; (h) $Ga(NO_3)_3$ or $^{67}GaCl_3$.

interest as an important target for the imaging and treatment of tumors. Several compounds with a high affinity for $\alpha_v\beta_3$ integrin have been investigated and developed.[13,14] Cyclic pentapeptides containing an RGD (arginine-glycine-aspartic acid) sequence are typical ligands for the $\alpha_v\beta_3$ integrin and have been investigated because of their high affinity. Radiolabeled RGD peptide-containing compounds have been used as tumor imaging agents for PET and SPECT.[15,16]

DOI: 10.1021/acs.bioconjchem.5b00186
Bioconjugate Chem. 2015, 26, 1561−1570

In the current study, we assumed that the introduction of a carrier to the tumor lesion, a carrier to bone metastases, and a stable gallium complex into one molecule could be a promising PET radiotracer using ^{68}Ga to detect both the primary lesion and bone metastases simultaneously. Based on this strategy, RGD peptide with high affinity for $\alpha_v\beta_3$ integrin, aspartic acid peptide for high affinity to hydroxyapatite in bone metastases, and Ga-1,4,7,10-tetraazacyclododecane-1,4,7,10-tetraacetic acid (DOTA) as a stable gallium complex were selected. The novel complexes, Ga-DOTA-D_8-c(RGDfK) and Ga-DOTA-D_{11}-c(RGDfK) (compounds **17** and **18** in Scheme 1) were designed, synthesized, and evaluated *in vitro* and *in vivo*. In this drug design, D_8 and D_{11} were selected because the sequence of more than eight aspartic acids in Ga-DOTA-D_n had demonstrated high affinity for bone in our previous study[8] and also because it is interesting to evaluate the effect of the introduction with different length of aspartic acid linkers in Ga-DOTA-D_n-c(RGDfK). The radiogallium complexes were prepared using the easy-to-handle radioisotope, ^{67}Ga rather than ^{68}Ga.

RESULTS

Preparation of the Radiogallium Complexes. Precursors were synthesized by the standard Fmoc-based solid-phase methodology according to Scheme 1, and the methods are described in Experimental Procedures.

The overall yields of the gallium complex precursors, DOTA-D_8-c(RGDfK), DOTA-D_{11}-c(RGDfK), and DOTA-c(RGDfK) were 2.3%, 3.3%, and 6.5%, respectively. The radiochemical yields of ^{67}Ga-DOTA-D_8-c(RGDfK), ^{67}Ga-DOTA-D_{11}-c(RGDfK), and ^{67}Ga-DOTA-c(RGDfK) were 93.6%, 92.4%, and 90.0%, respectively. After purification using HPLC, the radiochemical purities were all >97%. The retention times in HPLC chromatograms of ^{67}Ga-DOTA-D_n-c(RGDfK) (radioactivity) and Ga-DOTA-D_n-c(RGDfK) (UV absorbance) were almost the same (n = 0, 8, and 11). The comparable retention times in the chromatograms indicate that the radiolabeled products were identical to their nonradioactive counterparts, determined using mass spectrometry.

$\alpha_v\beta_3$ Integrin Binding Assay. The $\alpha_v\beta_3$ integrin binding affinities of the Ga-DOTA complex-conjugated c(RGDfK) peptides were determined using purified human $\alpha_v\beta_3$ integrin in a competitive binding assay with ^{125}I-c(RGDfK). Figure 1 shows typical ^{125}I-c(RGDfK) displacement curves achieved using Ga-DOTA-D_8-c(RGDfK), Ga-DOTA-D_{11}-c(RGDfK), Ga-DOTA-c(RGDfK), and c(RGDfK). The IC_{50} values (nM) of Ga-DOTA-D_8-c(RGDfK), Ga-DOTA-D_{11}-c(RGDfK), Ga-DOTA-c(RGDfK), and c(RGDfK) were 13.5 ± 5.6, 10.7 ± 1.9, 7.7 ± 1.8, and 15.1 ± 8.1, respectively. Because these values were similar (statistically not significant), the Ga-DOTA complex and the aspartic acid peptide linker did not significantly impede the affinity of c(RGDfK) peptide for $\alpha_v\beta_3$ integrin.

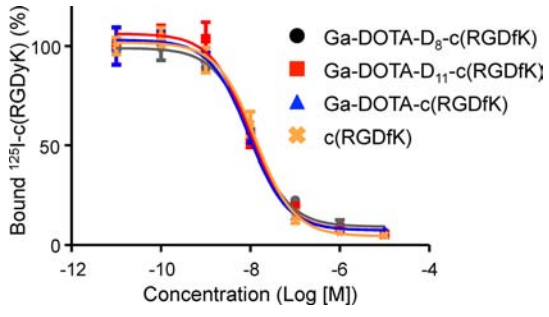

Figure 1. Typical displacement curves of competition binding assay to the $\alpha_v\beta_3$ integrin of ^{125}I-c(RGDyK) with Ga-DOTA-D_8-c(RGDfK), Ga-DOTA-D_{11}-c(RGDfK), Ga-DOTA-c(RGDfK), and c(RGDfK).

***In Vitro* Stability Experiments.** ^{67}Ga-DOTA-D_8-c(RGDfK), ^{67}Ga-DOTA-D_{11}-c(RGDfK), and ^{67}Ga-DOTA-c(RGDfK), which have the same DOTA ligand for chelating with gallium, exhibited same degree of stability in PBS (radiochemical purities (%) of 94.2 ± 3.2, 96.1 ± 2.8, and 94.6 ± 3.3 at 1 h, 91.7 ± 5.1, 92.4 ± 1.9, and 91.1 ± 2.0 at 3 h, and 84.8 ± 2.4, 87.4 ± 3.0, and 84.5 ± 2.3 at 24 h after incubation, respectively) and apo-transferrin solution (unbound ratios of radioactivity to apo-transferrin (%) of 97.5 ± 3.4, 96.1 ± 1.3, and 98.9 ± 1.0 at 1 h, 98.1 ± 0.5, 95.2 ± 1.3, and 96.7 ± 1.1 at 3 h, and 96.2 ± 3.7, 94.3 ± 1.2, and 95.1 ± 0.6 at 24 h, respectively). After incubation at 37 °C in PBS for 24 h, approximately 85% of the complexes remained intact. The results of incubation in apo-transferrin solution suggested that ^{67}Ga in the complexes was hardly taken away by apo-transferrin.

Hydroxyapatite Binding Assays. The binding ratios of ^{67}Ga-DOTA-D_8-c(RGDfK), ^{67}Ga-DOTA-D_{11}-c(RGDfK), ^{67}Ga-DOTA-c(RGDfK), and ^{67}Ga-DOTA to hydroxyapatite beads are shown in Figure 2. ^{67}Ga-DOTA and ^{67}Ga-DOTA-c(RGDfK), which do not contain an aspartic acid linker, did not bind to the hydroxyapatite significantly. In contrast, the percentage of ^{67}Ga-DOTA-D_8-c(RGDfK) and ^{67}Ga-DOTA-D_{11}-c(RGDfK) bound to the hydroxyapatite increased with increasing amounts of hydroxyapatite. ^{67}Ga-DOTA-D_{11}-c(RGDfK), which possesses a longer aspartic acid peptide linker, exhibited a higher binding ratio to the hydroxyapatite than did ^{67}Ga-DOTA-D_8-c(RGDfK).

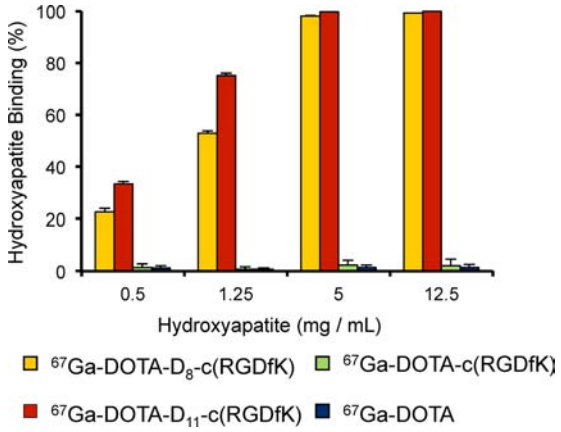

Figure 2. Binding ratios of ^{67}Ga-DOTA-D_8-c(RGDfK), ^{67}Ga-DOTA-D_{11}-c(RGDfK), ^{67}Ga-DOTA-c(RGDfK), and ^{67}Ga-DOTA to hydroxyapatite. Data are expressed as the mean ± SD for four samples.

***In Vitro* Protein Binding Studies.** The percentages of ^{67}Ga-DOTA-D_8-c(RGDfK), ^{67}Ga-DOTA-D_{11}-c(RGDfK), ^{67}Ga-DOTA-c(RGDfK), and $^{67}GaCl_3$ bound to proteins in mouse serum were 19.4% ± 5.8%, 17.0% ± 1.6%, 14.3% ± 3.5%, and 95.7% ± 0.9%, respectively. $^{67}GaCl_3$ showed significantly higher ratio of protein binding compared with ^{67}Ga-DOTA-D_n-c(RGDfK) compounds. Among ^{67}Ga-DOTA-D_n-c(RGDfK) compounds, the values of protein binding ratios were not significantly different.

DOI: 10.1021/acs.bioconjchem.5b00186
Bioconjugate Chem. 2015, 26, 1561−1570

Table 1. Biodistribution of Radioactivity at 1 h after Intravenous Administration of ^{67}Ga-DOTA-D_8-c(RGDfK), ^{67}Ga-DOTA-D_{11}-c(RGDfK), ^{67}Ga-DOTA-c(RGDfK), or $^{67}GaCl_3$ in U87MG Tumor Bearing Mice[a]

tissue	^{67}Ga-DOTA-D_8-c(RGDfK)	^{67}Ga-DOTA-D_{11}-c(RGDfK)	^{67}Ga-DOTA-c(RGDfK)	$^{67}GaCl_3$	blocking
blood	1.16(0.12)[c]	0.64(0.08)[c,d]	0.24(0.06)	17.87(1.56)	0.69(0.48)
liver	1.56(0.21)	1.57(0.13)	1.31(0.18)	4.76(0.24)	0.29(0.16)[e]
kidney	3.47(0.61)	2.89(0.59)	2.77(0.57)	5.59(0.60)	2.90(0.39)
small-intestine	2.26(0.72)	2.48(0.14)	1.76(0.45)	5.19(0.65)	1.47(0.59)[e]
large-intestine	0.92(0.14)	1.18(0.20)	1.17(0.17)	3.53(0.55)	0.38(0.12)[e]
spleen	1.28(0.09)	1.22(0.08)	1.17(0.21)	3.90(0.74)	0.24(0.10)[e]
pancreas	0.64(0.07)	0.79(0.07)[c,d]	0.50(0.08)	5.33(0.45)	0.31(0.20)[e]
lung	1.06(0.14)[c]	0.80(0.05)[c,d]	0.56(0.13)	10.77(0.69)	0.53(0.30)
heart	0.66(0.07)[c]	0.66(0.04)[c]	0.44(0.12)	4.86(0.29)	0.27(0.10)[e]
stomach[b]	0.76(0.24)[c]	0.56(0.06)[c,d]	0.29(0.06)	0.68(0.05)	0.66(0.09)[e]
bone	1.21(0.24)[c]	3.11(0.32)[c,d]	0.72(0.10)	11.96(1.41)	6.47(0.61)[e]
muscle	0.40(0.05)	0.46(0.05)[c]	0.36(0.03)	2.02(0.28)	0.14(0.07)[e]
brain	0.07(0.01)	0.08(0.01)	0.08(0.03)	0.55(0.02)	0.03(0.01)[e]
tumor	3.07(0.91)	2.83(1.38)	3.45(0.33)	10.57(2.69)	0.62(0.31)[e]

[a]Expressed as % injected dose per gram. Each value represents the mean (SD) for four animals. Blocking means biodistribution of radioactivity at 1 h after co-injection of ^{67}Ga-DOTA-D_{11}-c(RGDfK) with c(RGDfK) (0.2 mg/mouse) in U87MG tumor bearing mice. [b]Expressed as % injected dose. [c]$p < 0.05$ vs ^{67}Ga-DOTA-c(RGDfK). [d]$p < 0.05$ vs ^{67}Ga-DOTA-D_8-c(RGDfK). [e]$p < 0.05$ vs ^{67}Ga-DOTA-D_{11}-c(RGDfK).

Animal Experiments. The biodistribution of ^{67}Ga-DOTA-D_8-c(RGDfK), ^{67}Ga-DOTA-D_{11}-c(RGDfK), ^{67}Ga-DOTA-c-(RGDfK), and $^{67}GaCl_3$ is shown in Tables 1 and 2.

Table 2. Biodistribution of Radioactivity at 3 h after Intravenous Administration of ^{67}Ga-DOTA-D_8-c(RGDfK), ^{67}Ga-DOTA-D_{11}-c(RGDfK), ^{67}Ga-DOTA-c(RGDfK), or $^{67}GaCl_3$ in U87MG Tumor Bearing Mice[a]

tissue	^{67}Ga-DOTA-D_8-c(RGDfK)	^{67}Ga-DOTA-D_{11}-c(RGDfK)	^{67}Ga-DOTA-c(RGDfK)	$^{67}GaCl_3$
blood	0.86(0.09)[c]	0.37(0.03)[c,d]	0.14(0.03)	13.80(2.78)
liver	1.53(0.11)	2.67(0.22)[c,d]	1.66(0.17)	5.83(0.76)
kidney	2.80(0.31)[c]	2.95(0.25)[c]	2.21(0.10)	6.84(0.89)
small-intestine	1.24(0.38)[c]	2.53(0.35)[d]	2.06(0.47)	5.33(0.54)
large-intestine	2.25(0.29)[c]	4.53(0.24)[c,d]	2.90(0.36)	5.84(0.88)
spleen	1.25(0.11)	2.34(0.45)[c,d]	1.58(0.11)	4.93(1.43)
pancreas	0.44(0.04)[c]	0.47(0.06)[c]	0.25(0.04)	4.85(0.43)
lung	0.84(0.09)[c]	0.60(0.05)[d]	0.42(0.12)	9.11(0.80)
heart	0.49(0.05)[c]	0.57(0.04)[c]	0.33(0.05)	4.56(0.97)
stomach[b]	0.27(0.09)	0.33(0.06)	0.27(0.03)	0.77(0.09)
bone	2.28(0.22)[c]	4.55(0.53)[c,d]	0.79(0.09)	17.82(2.96)
muscle	0.25(0.05)[c]	0.29(0.01)[c]	0.16(0.04)	1.50(0.11)
brain	0.04(0.01)	0.04(0.00)	0.04(0.01)	0.38(0.05)
tumor	3.66(0.22)[c]	6.92(0.56)[c,d]	5.10(0.15)	9.81(1.55)

[a]Expressed as % injected dose per gram. Each value represents the mean (SD) for four animals. [b]Expressed as % injected dose. [c]$p < 0.05$ vs ^{67}Ga-DOTA-c(RGDfK). [d]$p < 0.05$ vs ^{67}Ga-DOTA-D_8-c(RGDfK).

The accumulation of ^{67}Ga-DOTA-D_{11}-c(RGDfK) in bone was significantly higher than that of ^{67}Ga-DOTA-D_8-c-(RGDfK). ^{67}Ga-DOTA-c(RGDfK) did not accumulate in bone appreciably. On the other hand, ^{67}Ga-DOTA-D_8-c(RGDfK), ^{67}Ga-DOTA-D_{11}-c(RGDfK), and ^{67}Ga-DOTA-c-(RGDfK) exhibited high uptake in tumor. Although the reason is unclear, the radioactivity in blood was slightly higher after the injection of ^{67}Ga-DOTA-D_8-c(RGDfK) than that after the injection of ^{67}Ga-DOTA-D_{11}-c(RGDfK) and ^{67}Ga-DOTA-c(RGDfK). The three radiogallium complexes exhibited similar biodistribution patterns in other organs, such as slightly high uptake in kidney, liver, intestine, and spleen and low uptake in pancreas, lung, heart, stomach, muscle, and brain.

$^{67}GaCl_3$ accumulated at high levels in bone and tumor. However, the radioactivity was also extremely high in blood and other organs. Thus, it would be difficult to use $^{68}GaCl_3$ as a PET tracer for tumor or bone imaging because of the short half-life of ^{68}Ga (68 min) and its delayed clearance from the blood and other nontargeted organs.

To evaluate the specificity of the novel gallium complex to $\alpha_v\beta_3$ integrin *in vivo*, the biodistribution of ^{67}Ga-DOTA-D_{11}-c(RGDfK) at 1 h after injection with an excess amount of RGD peptide is shown in Table 1 (blocking). A significantly reduced accumulation of ^{67}Ga-DOTA-D_{11}-c(RGDfK) in tumor was observed upon co-injection with c(RGDfK) peptide. The accumulation of radioactivity in most tissues (except bone) was decreased in the blocking experiment.

SPECT Images. Figure 3 shows axial (A, D, and G), sagittal (B, E, and H), and coronal (C, F, and I) views of SPECT images captured at 2 h after the injection of ^{67}Ga-DOTA-D_{11}, ^{67}Ga-DOTA-c(RGDfK), or ^{67}Ga-DOTA-D_{11}-c(RGDfK). The time point of SPECT imaging was set at 2 h postinjection of tracers. Considering the results of biodistribution experiments, imaging at a later time point should be better to obtain images of higher signal/noise ratios. However, because the application for the novel tracers to ^{68}Ga-PET is expected, imaging at an earlier time point should be better due to the short half-life of ^{68}Ga. ^{67}Ga-DOTA-D_{11} exhibited a marked accumulation of radioactivity in bone (Figure 3A–C). Very little accumulated radioactivity was observed in tissues other than bone, confirming the results of the biodistribution experiments in our previous report.[8] ^{67}Ga-DOTA-c(RGDfK) showed a high accumulation of radioactivity surrounding the site of tumor cell inoculation. Although kidney, which is the route of excretion, also exhibited the accumulation of relatively high amounts of radioactivity, the accumulation of radioactivity was lower in the other tissues, including bone. In contrast, ^{67}Ga-DOTA-D_{11}-c(RGDfK) exhibited high accumulation of radioactivity in both tumor and bone, which is consistent with the biodistribution experiments.

DOI: 10.1021/acs.bioconjchem.5b00186
Bioconjugate Chem. 2015, 26, 1561–1570

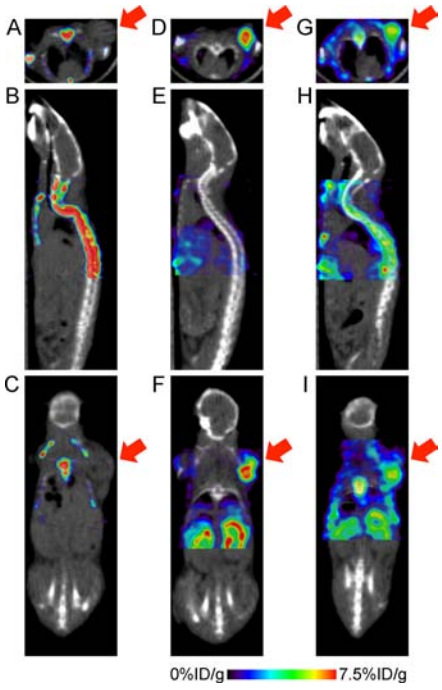

Figure 3. SPECT/CT images (A, D, G, axial images; B, E, H, sagittal images; C, F, I, coronal images) of tumor bearing mice at 2 h after the intravenous injection of (A–C) ^{67}Ga-DOTA-D$_{11}$, (D–F) ^{67}Ga-DOTA-c(RGDfK), or (G–I) ^{67}Ga-DOTA-D$_{11}$-c(RGDfK). Arrows indicate the site where tumor cells were injected.

DISCUSSION

The purpose of this study was to develop a PET tracer that could detect osteoblastic bone metastases, primary cancer, and osteolytic metastases simultaneously. To achieve this, a stable gallium complex site for a PET radionuclide, an aspartic acid peptide linker as a carrier to osteoblastic bone metastases, and an RGD peptide sequence as a carrier to the primary cancer and osteolytic metastases were introduced into one molecule.

^{68}Ga is one of the most practical and interesting radionuclides for clinical PET because ^{68}Ga is an in-house generator-produced radionuclide that can be eluted at any time on-demand. The easy labeling of short half-life radionuclides is very important for clinical use. Although any differences between ^{68}Ga and ^{67}Ga for labeling DOTA derivatives are unclear, the radiochemical yields were very high (>90%) in the current study. The next step for their clinical use is to optimize the labeling conditions using ^{68}Ga to obtain higher radiochemical yields at low ligand concentration. Then, preparation of a kit for radiolabeling that does not require purification should be tested.

In stability experiments *in vitro*, the results indicated that the radiogallium complexes were slowly decomposed in a time-dependent manner in PBS and were hardly taken away by apotransferrin. The slight decomposition should not be critical problem. ^{67}Ga-DOTA-D$_n$-c(RGDfK) complexes showed fast blood clearance and free gallium (^{67}GaCl$_3$) showed very slow blood clearance (Tables 1 and 2). The protein binding ratios of ^{67}Ga-DOTA-D$_n$-c(RGDfK) complexes were low, and the protein binding ratio of ^{67}GaCl$_3$ was extremely high from the results of *in vitro* protein binding experiments. Then, if ^{67}Ga was released from ^{67}Ga-DOTA-D$_n$-c(RGDfK), the blood clearance of radioactivity after injection of ^{67}Ga-DOTA-D$_n$-c(RGDfK) could be delayed. Moreover, if any peptide bonds in ^{67}Ga-DOTA-D$_n$-c(RGDfK) were cleaved, tumor accumulation of radioactivity could be lower. Therefore, these results indicated that large proportions of ^{67}Ga-DOTA-D$_n$-c(RGDfK) complexes were distributed to whole body without decomposition. Meanwhile, the blood clearance of radioactivity after injection of ^{67}Ga-DOTA-D$_n$-c(RGDfK) was correlated with the protein binding ratios of ^{67}Ga-DOTA-D$_n$-c(RGDfK) although the difference of the protein binding ratios among ^{67}Ga-DOTA-D$_n$-c(RGDfK) complexes was not significant. The protein binding does not always decide the blood clearance, but there is no conflict between the blood clearance in the biodistribution experiments and the results of the protein binding experiments *in vitro*.

Recent reports suggested that aspartic acid-containing peptides could be useful carriers for bone imaging radiotracers.[8,17] The affinity of aspartic acid peptides for bone is derived from the high affinity of the acidic amino acid peptides for hydroxyapatite in bone,[18,19] which is similar to that of the bisphosphonate compounds that have been used as carriers for bone-seeking radiopharmaceuticals. In the current study, ^{67}Ga-DOTA and ^{67}Ga-DOTA-c(RGDfK), which do not contain an aspartic acid peptide linker, did not bind to hydroxyapatite significantly, whereas, ^{67}Ga-DOTA-D$_8$-c(RGDfK) and ^{67}Ga-DOTA-D$_{11}$-c(RGDfK), which possess an aspartic acid peptide linker, exhibited a high affinity for hydroxyapatite, as expected (Figure 2). Thus, in the current drug design, the aspartic acid peptide linker between the Ga-DOTA complex and the RGD peptide could function as a carrier to bone. In SPECT imaging, ^{67}Ga-DOTA-D$_{11}$-c(RGDfK) exhibited a high accumulation of radioactivity in bone (Figure 3G–I), whereas ^{67}Ga-DOTA-c(RGDfK) did not accumulate in bone (Figure 3D–F). Moreover, our recent report demonstrated that the affinity for hydroxyapatite increased as the number of aspartic acid residues increased.[8] Therefore, the results of the hydroxyapatite binding assays and biodistribution experiments demonstrated that the affinity for bone was increased as the number of aspartic acid residues increased [Figure 2, Tables 1 and 2; ^{67}Ga-DOTA-c(RGDfK) < ^{67}Ga-DOTA-D$_8$-c(RGDfK) < ^{67}Ga-DOTA-D$_{11}$-c(RGDfK)]. It was reported that the bone accumulation of ^{67}Ga-DOTA-D$_{14}$ was not higher than that of ^{67}Ga-DOTA-D$_{11}$ in our recent paper.[8] Thus, ^{67}Ga-DOTA-D$_{14}$-c(RGDfK) was not prepared in this study. But, in the case of ^{67}Ga-DOTA-D$_n$-c(RGDfK), since the c(RGDfK) structure and ^{67}Ga-DOTA structure could be a structural obstacle to access of the D$_n$ site to hydroxyapatite, the length of D$_{11}$ may be not enough for higher bone accumulation of ^{67}Ga-DOTA-D$_n$-c(RGDfK). The result that the bone accumulation of ^{67}Ga-DOTA-D$_{11}$ was significantly higher than that of ^{67}Ga-DOTA-D$_{11}$-c(RGDfK) also supports the hypothesis. ^{67}Ga-DOTA-D$_{14}$-c(RGDfK) should be prepared and evaluated in the next study.

Bone scintigraphic radiotracers in clinical practice, which consist of ^{99m}Tc complexes with bisphosphonate to serve as a carrier to bone, have been used widely to diagnose metabolic bone diseases such as cancer bone metastases. In particular, ^{99m}Tc-bisphosphonate complexes accumulate at high levels in lesions with high osteoblastic activity because the newly formed bone has a much larger surface area (since the crystalline structure of hydroxyapatite in the newly formed bone is amorphous and has a greater surface area) than does the normal bone.[20] Accordingly, it could be predicted that ^{67}Ga-DOTA-D$_{11}$-c(RGDfK), which has an aspartic acid linker with high affinity for hydroxyapatite as well as the bisphosphonate

DOI: 10.1021/acs.bioconjchem.5b00186
Bioconjugate Chem. 2015, 26, 1561–1570

carrier, would also exhibit high accumulation in high osteoblastic activity lesions, such as osteoblastic bone metastatic lesions, in bone tissue. Meanwhile, the sensitivity and the accuracy of ^{99m}Tc-bisphosphonate complexes in patients with osteolytic bone metastases are lower than those of [^{18}F]FDG, which is the gold standard for tumor imaging using clinical PET, because ^{99m}Tc-bisphosphonate complexes do not accumulate well in osteolytic lesions.[21] To develop a radiotracer to accumulate in osteolytic bone metastatic lesions, Wadas et al. reported that a radiolabeled RGD peptide (^{64}Cu-RGD) targeting $\alpha_v\beta_3$ integrin could be used to visualize osteolytic bone metastases in an animal model[22] since $\alpha_v\beta_3$ integrin is expressed abundantly on the surface of angiogenic blood vessels, certain tumor cells, and osteoclasts,[23,24] which are abundant in lesions with high osteolytic activity. Zheleznyak et al. also demonstrated that the ^{64}Cu-RGD could image the increased osteoclastogenesis that is typically associated with pathologically active bone resorption *in vivo*.[25] In addition, Miao et al. reported that another ^{99m}Tc-labeled RGD peptide exhibited the higher specificity and accuracy in lung cancer patients with bone metastases compared with ^{99m}Tc-MDP bone scintigraphy.[26] Accordingly, it is likely that $\alpha_v\beta_3$ integrin is the target molecule and RGD peptide is the carrier to osteolytic bone metastases. Ga-DOTA-D$_n$-c(RGDfK), which contains c(RGDfK), has a high affinity for $\alpha_v\beta_3$ integrin *in vitro* (Figure 1). Thus, Ga-DOTA-D$_n$-c(RGDfK) is also expected to accumulate in osteolytic bone metastases. Moreover, it was reported that RGD peptide could also be a carrier to primary cancers;[27−29] therefore, Ga-DOTA-D$_n$-c(RGDfK), which contains an aspartic acid peptide linker and c(RGDfK), could accumulate in primary tumor, osteoblastic bone metastases, and osteolytic bone metastases simultaneously because the RGD peptide site is responsible for radioactivity localization in primary tumor and osteolytic bone metastases lesions, and the aspartic acid peptide linker is responsible for radioactivity localization in osteoblastic bone metastases. Although the current study confirmed that Ga-DOTA-D$_{11}$-c(RGDfK) accumulated in tumor and bone by biodistribution experiments and SPECT imaging in U87MG tumor-bearing mice, the accumulation in bone metastases was not confirmed. The accumulation of Ga-DOTA-D$_{11}$-c(RGDfK) in bone metastases should be confirmed in bone metastasis animal models in the near future.

In the current study, a blocking experiment was performed to confirm the specific accumulation of the radiotracer. The accumulation of ^{67}Ga-DOTA-D$_{11}$-c(RGDfK) in tumor was reduced significantly by the co-injection of an excess amount of RGD peptide, which suggests that the tumor accumulation of ^{67}Ga-DOTA-D$_{11}$-c(RGDfK) is caused by the specific binding affinity of the c(RGDfK) motif to $\alpha_v\beta_3$ integrin. Moreover, the reduced radioactivity of ^{67}Ga-DOTA-D$_{11}$-c(RGDfK) in all tissues except kidney and bone by the co-injection of RGD peptide was consistent with previous radiolabeled RGD studies without accumulation in bone.[30] The c(RGDfK) motif in ^{67}Ga-DOTA-D$_{11}$-c(RGDfK) should also affect the reduction in radioactivity. In contrast, although the bone accumulation of labeled RGD peptides tended to be decreased by the co-injection of RGD peptide in previous reports, the bone accumulation of ^{67}Ga-DOTA-D$_{11}$-c(RGDfK) was significantly increased by co-injection of RGD peptide. This suggests that the accumulation of ^{67}Ga-DOTA-D$_{11}$-c(RGDfK) in bone is caused by the aspartic acid linker, not the c(RGDfK) motif.

The drug design concept that includes a radiometal complex-conjugated RGD peptide with an aspartic acid peptide linker is applicable to both diagnosis and therapy. Radiolabeled RGD peptides with a β emitter radionuclide, such as yttrium (^{90}Y) or lutetium (^{177}Lu), have been applied to radionuclide therapy and showed promising results.[31,32] For bone-seeking agents, some therapeutic radiopharmaceuticals labeled with α- or β-emitting radionuclides have been approved for the palliation of bone metastases, and many labeled compounds have been developed and studied in basic research.[33−37] Therefore, combination peptides could be applicable to radionuclide therapy. In the current study, we selected DOTA as the ligand and introduced it into the designed compound, and the Ga-DOTA complexes demonstrated high stability in buffered solution. For gallium labeling, 1,4,7-triazacyclononane-triacetic acid (NOTA) or triazacyclononane-phosphinate (TRAP) may be better ligands because they could be radiolabeled with high yields of radiogallium using lower concentrations of precursors.[38] However, since DOTA ligands could form a stable complex with not only gallium ($^{67/68}$Ga) but also indium (^{111}In), yttrium (^{90}Y), lutetium (^{177}Lu), and bismuth (^{213}Bi), DOTA-D$_{11}$-c(RGDfK) could also be labeled with these radiometals. Therefore, DOTA may be more beneficial in radionuclide therapy applications than NOTA or TRAP. Generally, if radiometal complexes are stable, different complexes labeled using the same precursor with different radiometals are expected to have a similar biodistribution. Therefore, DOTA-D$_{11}$-c(RGDfK) could be useful for a coupling diagnosis and therapy by labeling with diagnostic radionuclides and therapeutic radionuclides, namely theranostics.

■ CONCLUSIONS

The present study suggests that ^{68}Ga-DOTA-D$_{11}$-c(RGDfK), which contains ^{68}Ga instead of ^{67}Ga, has great potential as a PET tracer for the diagnosis of primary cancer lesions as well as osteoblastic and osteolytic bone metastases simultaneously. This could provide useful information for the development of diagnostic and therapeutic radiolabeled compounds and a coupling method between diagnosis and therapy, namely theranostics, for future research.

■ EXPERIMENTAL PROCEDURES

Electrospray ionization mass spectra (ESI-MS) were obtained with JEOL JMS-T100TD (JEOL Ltd., Tokyo, Japan). Matrix assisted laser desorption/ionization-time-of-flight mass spectra (MALDI-TOF-MS) were obtained with ABI 4800 plus (AB SCIEX, Foster, CA, USA). $^{67}GaCl_3$ is kindly provided by Nihon Medi-physics (Tokyo, Japan). [^{125}I]NaI (644 GBq/mg) was purchased from PerkinElmer (Waltham, MA, USA). 1,4,7,10-Tetraazacyclododecane-1,4,7-tris(*t*-butyl acetate) (DOTA-tris) was purchased from Macrocyclics (Dallas, TX, USA). U87MG glioblastoma cells were purchased from DS Pharma Biomedical (Osaka, Japan). Other chemicals and solvents were all of reagent grade and used without further purification.

Synthesis of Precursors. Cyclic[Arg(Pmc)-Gly-Asp-(OtBu)-D-Phe-Lys(Alloc)] (**3**) was synthesized manually by the standard Fmoc-based solid-phase methodology. Namely, Fmoc-Gly-OH (4 mol equiv to resin) was dissolved in dichloromethane. 2-Chlorotrityl chloride resin and *N*,*N*-diisopropylethylamine (DIEA, 3.5 equiv) were added. The reaction mixture was rotated for 1 h, and 1 mL of methanol was added to further react for 30 min at room temperature. The

DOI: 10.1021/acs.bioconjchem.5b00186
Bioconjugate Chem. 2015, 26, 1561−1570

peptide chain was constructed according to the cycle consisting of (a) 15 min deprotection of Fmoc group with 20% piperidine in *N*,*N*-dimethylformamide (DMF) and (b) 1.5 h coupling of the Fmoc-Arg(Pmc)-OH, Fmoc-Lys(Alloc)-OH, Fmoc-D-Phe-OH, and Fmoc-Asp(OtBu)-OH (2.5 equiv) with 1,3-diisopropylcarbodiimide (DIPCI, 2.5 equiv) and 1-hydroxybenzotriazole hydrate (HOBt, 2.5 equiv) in DMF. The coupling reaction was repeated when the resin became positive to the Kaiser test to obtain Resin-Gly-Arg(Pmc)-Lys(Alloc)-D-Phe-Asp(OtBu) (**1**).

The resin-bound peptide was treated with 30% 1,1,1,3,3,3-hexafluoro-2-propanol (HFIP) in dichloromethane for 5 min to cleave the bond between the resin and the peptide. After filtration, the solvent in the filtrate was removed *in vacuo*. The residue, crude Gly-Arg(Pmc)-Lys(Alloc)-D-Phe-Asp(OtBu) (**2**), was used in the next reaction without further purification. The peptide was dissolved in DMF (5 mM), and then $NaHCO_3$ (5 equiv) and diphenylphosphoryl azide (DPPA, 3 equiv) were added. After 24 h stirring at room temperature, the solid $NaHCO_3$ was removed by filtration, and DMF was removed *in vacuo*. The residue, crude cyclic[Gly-Arg(Pmc)-Lys(Alloc)-D-Phe-Asp(OtBu)] (**3**), was used in the next reaction without further purification.

The Alloc protecting group of the ε amino group in lysine was selectively deprotected by the treatment of $Pd(PPh_3)_4$ in chloroform/acetic acid/*N*-methylmorpholine (37:2:1) for 2 h under a N_2 atmosphere. The crude peptide was purified by reversed phase (RP)-HPLC on Cosmosil $5C_{18}$-AR-300 column (10 mm × 150 mm; Nacalai Tesque, Kyoto, Japan) at a flow rate of 4.0 mL/min with a gradient mobile phase of 55% methanol in water with 0.1% trifluoroacetic acid (TFA) to 75% methanol in water with 0.1% TFA for 20 min (gradient system A). Chromatograms were obtained by monitoring the UV absorption at a wavelength of 220 nm. The fraction containing cyclic[Arg(Pmc)-Gly-Asp(OtBu)-D-Phe-Lys] was determined by mass spectrometry and collected. The solvents were removed by lyophilization to provide cyclic[Arg(Pmc)-Gly-Asp(OtBu)-D-Phe-Lys] (**4**, 98.8 mg, 53.3%) as a yellow powder.

Cyclic[Arg(Pmc)-Gly-Asp(OtBu)-D-Phe-Lys]: RP-HPLC (gradient system A, t_R = 14.9 min), ESI-MS (*m*/*z* calcd for $C_{45}H_{68}N_9O_{10}S$ ($[M + H]^+$) 926.5, found 926.4).

DOTA(tris)-$[Asp(OtBu)]_8$ (**9**) and DOTA(tris)-$[Asp(OtBu)]_{11}$ (**10**) were synthesized by Fmoc solid-phase methodology using the above-mentioned procedure and used in the next reaction without further purification.

Cyclic[Arg(Pmc)-Gly-Asp(OtBu)-D-Phe-Lys] (**4**, 9.25 mg, 10.0 μmol) and DOTA(tris)-$[Asp(OtBu)]_{11}$ (**10**, 24.6 mg, 10.0 μmol) were dissolved in 500 μL of DMF. HOBt (8 equiv) and DIPCI (7 equiv) were added to the reaction mixture. The reaction solution was shaken gently for 2 h, then purified by RP-HPLC on Cosmosil $5C_{18}$-AR-300 column (10 mm × 150 mm) at a flow rate of 4.0 mL/min with a gradient mobile phase of 70% methanol in water with 0.1% TFA to 100% methanol in water with 0.1% TFA for 20 min (gradient system B). Chromatograms were obtained by monitoring the UV absorption at a wavelength of 220 nm. The fraction containing DOTA(tris)-$[Asp(OtBu)]_{11}$-cyclic[Arg(Pmc)-Gly-Asp(OtBu)-D-Phe-Lys] (**12**) was determined by mass spectrometry and collected. The solvent was removed by lyophilization to provide a white powder (24.0 mg, 71.4%).

DOTA(tris)-$[Asp(OtBu)]_8$-cyclic[Arg(Pmc)-Gly-Asp(OtBu)-D-Phe-Lys] (**11**, 12.4 mg, 43.5%) was obtained by the above-mentioned method using the DOTA(tris)-$[Asp(OtBu)]_8$ (**9**) as a starting material instead of DOTA(tris)-$[Asp(OtBu)]_{11}$ (**10**).

DOTA(tris)-cyclic[Arg(Pmc)-Gly-Asp(OtBu)-D-Phe-Lys] (**13**, 6.8 mg, 45.9%) was obtained by the same method as DOTA(tris)-$[Asp(OtBu)]_{11}$-cyclic[Arg(Pmc)-Gly-Asp(OtBu)-D-Phe-Lys] (**12**) using the DOTA(tris) as a starting material instead of DOTA(tris)-$[Asp(OtBu)]_{11}$ (**10**).

DOTA(tris)-cyclic[Arg(Pmc)-Gly-Asp(OtBu)-D-Phe-Lys]: RP-HPLC (gradient system B, t_R = 8.5 min), ESI-MS (*m*/*z* calcd for $C_{73}H_{118}N_{13}O_{17}S$ ($[M + H]^+$) 1480.8, found 1480.9).

DOTA(tris)-$[Asp(OtBu)]_8$-cyclic[Arg(Pmc)-Gly-Asp(OtBu)-D-Phe-Lys]: RP-HPLC (gradient system B, t_R = 13.9 min), ESI-MS (*m*/*z* calcd for $C_{137}H_{222}N_{21}O_{41}S$ ($[M + H]^+$) 2850.6, found 2850.6).

DOTA(tris)-$[Asp(OtBu)]_{11}$-cyclic[Arg(Pmc)-Gly-Asp(OtBu)-D-Phe-Lys]: RP-HPLC (gradient system B, t_R = 15.5 min), ESI-MS (*m*/*z* calcd for $C_{161}H_{261}N_{24}O_{50}S$ ($[M + H]^+$) 3363.8, found 3363.9).

DOTA(tris)-$[Asp(OtBu)]_{11}$-cyclic[Arg(Pmc)-Gly-Asp(OtBu)-D-Phe-Lys] (**12**) was treated with a mixture of 95% TFA, 2.5% water, and 2.5% triisopropylsilane (TIS) for 24 h at room temperature. The crude peptide was purified by reversed phase RP-HPLC on Cosmosil $5C_{18}$-AR-II column (4.6 mm × 150 mm) at a flow rate of 1.0 mL/min with a gradient mobile phase of 10% methanol in water with 0.1% TFA to 50% methanol in water with 0.1% TFA for 20 min (gradient system C). Chromatograms were obtained by monitoring the UV absorption at a wavelength of 220 nm. The solvent was removed by lyophilization to provide DOTA-D_{11}-c(RGDfK) (**15**, 1.54 mg, 11.1%) as a white powder.

Deprotection of DOTA(tris)-$[Asp(OtBu)]_8$-cyclic[Arg(Pmc)-Gly-Asp(OtBu)-D-Phe-Lys] and DOTA(tris)-cyclic[Arg(Pmc)-Gly-Asp(OtBu)-D-Phe-Lys] was performed by the same method. DOTA-D_8-c(RGDfK) (**14**, 1.20 mg, 22.3%) and DOTA-c(RGDfK) (**16**, 1.20 mg, 26.4%) were obtained.

DOTA-c(RGDfK): RP-HPLC (gradient system C, t_R = 12.8 min), ESI-MS (*m*/*z* calcd for $C_{43}H_{68}N_{13}O_{14}$ ($[M + H]^+$) 990.5, found 990.5).

DOTA-D_8-c(RGDfK): RP-HPLC (gradient system C, t_R = 14.9 min), MALDI-TOF-MS (*m*/*z* calcd for $C_{75}H_{108}N_{21}O_{38}$ ($[M + H]^+$) 1910.7, found 1910.7).

DOTA-D_{11}-c(RGDfK): RP-HPLC (gradient system C, t_R = 16.6 min), MALDI-TOF-MS (*m*/*z* calcd for $C_{87}H_{123}N_{24}O_{47}$ ($[M + H]^+$) 2255.8, found 2255.9).

Preparation of Nonradioactive Gallium Complexes. $Ga(NO_3)_3$ (3.6 mg, 14.1 μmol) was dissolved in 360 μL of water. DOTA-D_{11}-c(RGDfK) (**15**) (1.1 mg, 0.488 μmol) was dissolved in 96 μL of water and mixed with 48 μL of the $Ga(NO_3)_3$ solution. The mixture was heated for 2 h at 40 °C and purified by HPLC to give Ga-DOTA-D_{11}-c(RGDfK) (**18**) (1.08 mg, 95.4%). RP-HPLC was carried on Cosmosil $5C_{18}$-AR-II (4.6 mm × 150 mm) at a flow rate of 1 mL/min with a gradient mobile phase of 15% methanol in water with 0.1% TFA to 40% methanol in water with 0.1% TFA for 30 min (gradient system D).

DOTA-D_8-c(RGDfK) (**14**, 1.0 mg, 0.524 μmol) and DOTA-c(RGDfK) (**16**, 0.60 mg, 0.606 μmol) were reacted with $Ga(NO_3)_3$ and purified by the above-mentioned method to give Ga-DOTA-D_8-c(RGDfK) (**17**, 0.93 mg, 89.9%) and Ga-DOTA-c(RGDfK) (**19**, 0.56 mg, 87.5%)

DOI: 10.1021/acs.bioconjchem.5b00186
Bioconjugate Chem. 2015, 26, 1561−1570

Ga-DOTA-c(RGDfK): RP-HPLC (gradient system D, t_R = 12.5 min), ESI-MS (m/z calcd for $C_{43}H_{65}GaN_{13}O_{14}$ ($[M]^+$) 1056.4, found 1056.4).

Ga-DOTA-D_8-c(RGDfK): RP-HPLC (gradient system D, t_R = 17.0 min), MALDI-TOF-MS (m/z calcd for $C_{75}H_{105}GaN_{21}O_{38}$ ($[M]^+$) 1976.6, found 1976.7).

Ga-DOTA-D_{11}-c(RGDfK): RP-HPLC (gradient system D), t_R = 18.5 min, MALDI-TOF-MS (m/z calcd for $C_{87}H_{120}GaN_{24}O_{47}$ ($[M]^+$) 2321.7, found 2321.8).

$\alpha_v\beta_3$ Integrin Binding Assay. Binding affinities of synthesized peptides for $\alpha_v\beta_3$ receptor were determined according to procedures reported previously with a slight modification.[39] Plates (96-well; Thermo, Waltham, MA, USA) were coated with 100 μL/well of a purified human integrin $\alpha_v\beta_3$ solution (600 ng/mL, Chemicon-Millipore, Billerica, MA, USA) in coating buffer (25 mM Tris-HCl pH 7.4, 150 mM NaCl, 1 mM $CaCl_2$, 0.5 mM $MgCl_2$, and 1 mM $MnCl_2$) for 17 h at 4 °C. The plates were washed twice with binding buffer [containing 0.1% bovine serum albumin (BSA) in coating buffer]. The wells were blocked for 2 h with 200 μL blocking buffer (containing 1% BSA in coating buffer). The plates were washed twice with binding buffer. Then, 95 μL of binding buffer containing 22 kBq of ^{125}I-c(RGDyK), which was prepared by chloramine T method with c(RGDyK) peptide and purified by HPLC, and 5 μL of binding buffer containing various concentrations of Ga-DOTA-D_8-c(RGDfK), Ga-DOTA-D_{11}-c(RGDfK), Ga-DOTA-c(RGDfK), or c(RGDfK) were added and incubated at 37 °C for 1 h. After incubation, the plates were washed three times with the binding buffer and were counted in a γ counter (ARC-7010B, Hitachi Aloka Medical, Ltd., Tokyo, Japan). The half maximal inhibitory concentration (IC_{50}) values of the peptides were calculated by curve fitting with nonlinear regression using GraphPad Prism 5.04 (GraphPad Software Inc., San Diego, CA, USA). Each data point is the average of four determinations, and IC_{50} values were expressed as the mean ± standard deviation (SD) from three independent experiments.

Radiolabeling with ^{67}Ga. A precursor, DOTA-D_{11}-c(RGDfK) (20 μg), was dissolved in 75 μL of 0.2 M ammonium acetate buffer (pH 5.0), and then 25 μL of $^{67}GaCl_3$ (74 MBq/mL) solution was added to the solution. After heating for 8 min at 80 °C, the solution was purified by RP-HPLC (gradient system D).

Precursors DOTA-D_8-c(RGDfK) and DOTA-c(RGDfK) were radiolabeled with ^{67}Ga and purified by the above-mentioned method.

***In Vitro* Stability Experiments.** ^{67}Ga-DOTA-D_8-c(RGDfK), ^{67}Ga-DOTA-D_{11}-c(RGDfK), and ^{67}Ga-DOTA-c(RGDfK) were incubated in 0.1 M phosphate buffered saline (PBS, pH 7.4) for 24 h at 37 °C. The solutions after incubation of 1, 3, and 24 h were analyzed by RP-HPLC.

The tracers were incubated in 1 M PBS (pH 7.4) containing 7.5 mg/mL apo-transferrin. The solutions were incubated for 24 h at 37 °C. The solution at 1, 3, and 24 h after incubation was analyzed by size-exclusion HPLC analysis on a TSK-GEL Super SW3000 column (4.6 mm × 300 mm, TOSOH, Tokyo, Japan) at a flow rate of 0.3 mL/min with an isocratic mobile phase of 0.1 M PBS (pH 6.8).

Hydroxyapatite Binding Assays. Experiments for hydroxyapatite binding were performed according to procedures reported previously with a slight modification.[35,40] In brief, hydroxyapatite beads (Bio-Gel; Bio-Rad, Hercules, CA, USA) were suspended in Tris/HCl-buffered saline (50 mM, pH 7.4) at 1, 2.5, 10, or 25 mg/mL. Two hundred microliters of each solution of ^{67}Ga-labeled peptide and ^{67}Ga-DOTA was added to 200 μL of hydroxyapatite suspension. Corresponding precursors were added to the suspension to adjust the ligand concentrations to 19.5 μM. The mixture was gently shaken for 1 h at room temperature. After centrifugation at 10000g for 5 min, the radioactivity of the supernatant was measured. Control group was performed using the same procedure without hydroxyapatite beads. The rate of hydroxyapatite binding was determined using the following equation.

$$\text{Hydroxyapatite binding rate (\%)} = (1 - [\text{radioactivity of supernatant of each sample}] / [\text{radioactivity of supernatant of control}]) \times 100$$

***In Vitro* Protein Binding Studies.** The protein binding ratios of ^{67}Ga-DOTA-D_8-c(RGDfK), ^{67}Ga-DOTA-D_{11}-c(RGDfK), ^{67}Ga-DOTA-c(RGDfK), and $^{67}GaCl_3$ were evaluated by ultrafiltration (Amicon ultra centrifugal filters, 0.5 mL, 30K membrane; Millipore, Billerica, MA, USA) according to the protocol described in a previous report with a slight modification.[41] Each tracer (6−19 kBq in 10 μL saline) was added to 90 μL of mouse serum. Mixtures (90 μL) of each tracer and serum were centrifuged at 14000g for 20 min at room temperature. The radioactivity of the initial mixtures (10 μL) and the filtrates (10 μL) was measured. Free fraction ratio and protein binding ratio were determined as follows:

$$\text{Free fraction ratio (\%)} = (\text{radioactivity of filtrate}) / (\text{radioactivity of initial}) \times 100$$

$$\text{Protein binding ratio (\%)} = 100 - (\text{Free fraction ratio})$$

Biodistribution Experiments. Experiments with animals were conducted in strict accordance with the Guidelines for the Care and Use of Laboratory Animals of Kanazawa University. The animal experimental protocols used were approved by the Committee on Animal Experimentation of Kanazawa University (Permit Number AP-132633). The animals were housed with free access to food and water at 23 °C with a 12-h alternating light/dark schedule. To produce tumors, approximately 5 × 10^6 of the prepared U87MG glioblastoma cells in 100 μL of PBS were injected subcutaneously into the right and left shoulders of 4-week-old female BALB/c nude mice (15−19 g, Japan SLC, Inc., Hamamatsu, Japan). Biodistribution experiments were performed approximately 14−21 days postinoculation, that is, the time needed for tumors to reach a palpable size. Groups of four mice at each time point were intravenously administered 100 μL of saline solution of ^{67}Ga-DOTA-D_8-c(RGDfK), ^{67}Ga-DOTA-D_{11}-c(RGDfK), ^{67}Ga-DOTA-c(RGDfK), or $^{67}GaCl_3$ (37−148 kBq). Mice were sacrificed at 1 and 3 h postinjection. Tissues of interest were removed and weighed. Complete left femurs were isolated as representative bone samples, radioactivity counts were determined with an auto well γ counter, and counts were corrected for background radiation and physical decay during counting.

To investigate the effect of an excess amount of RGD peptide on biodistribution, U87MG tumor bearing mice were intravenously administered 100 μL of a mixed solution of ^{67}Ga-DOTA-D_{11}-c(RGDfK) (74 kBq) and c(RGDfK) peptide (0.2

DOI: 10.1021/acs.bioconjchem.5b00186
Bioconjugate Chem. 2015, 26, 1561−1570

mg/mouse). Mice (n = 4) were sacrificed at 1 h postinjection, and biodistribution experiments were conducted as described above.

SPECT Imaging. Tumor-bearing mice for imaging were prepared by the above-mentioned method with a slight modification, namely, U87MG cells were injected subcutaneously into only the right shoulder of mice. Micro-SPECT/CT imaging was performed approximately 21 days postinoculation, that is, the time needed for tumors to reach a palpable size (0.7−1.0 cm in diameter). At 2 h after injection of ^{67}Ga-DOTA-D$_{11}$, which was prepared by the described method previously,[8] ^{67}Ga-DOTA-c(RGDfK), or ^{67}Ga-DOTA-D$_{11}$-c(RGDfK) (4.9−7.9 MBq/mouse) into tumor-bearing mice, mice were sacrificed because of long time acquisition of SPECT imaging. SPECT and X-ray CT images of a mouse for each tracer were performed by the eXplore speCZT CT 120 (GE Healthcare, Milwaukee, WI, USA). SPECT data acquisition was performed in 1000−1300 s/frame for 50 frames. The energy window was 65−210 keV.

Statistical Analysis. Data are expressed as means ± standard deviations. Significance for half maximal inhibitory concentration (IC_{50}) values in integrin binding assays and biodistribution experiments among ^{67}Ga-DOTA-D$_8$-c(RGDfK), ^{67}Ga-DOTA-D$_{11}$-c(RGDfK), and ^{67}Ga-DOTA-c(RGDfK) was determined using a one-way analysis of variance (ANOVA) followed by the Tukey−Kramer post hoc test. Significance for *in vitro* protein binding experiments among ^{67}Ga-DOTA-D$_8$-c(RGDfK), ^{67}Ga-DOTA-D$_{11}$-c(RGDfK), ^{67}Ga-DOTA-c(RGDfK), and $^{67}GaCl_3$ was also determined using a one-way analysis of variance (ANOVA) followed by the Tukey−Kramer post hoc test. Significance between biodistribution data of ^{67}Ga-DOTA-D$_{11}$-c(RGDfK) and its blocking data by co-injection with c(RGDfK) peptide was determined using unpaired Student's t test. Results were considered statistically significant at $p < 0.05$.

AUTHOR INFORMATION

Corresponding Author

*Mailing address: Division of Pharmaceutical Sciences; Graduate School of Medical Sciences; Kanazawa University; Kakuma-machi, Kanazawa 920-1192, Japan. Telephone: 81-76-234-4460. Fax: 81-76-234-4459 .E-mail: kogawa@p.kanazawa-u.ac.jp.

Notes

The authors declare no competing financial interest.

ACKNOWLEDGMENTS

This work was supported in part by Sagawa Foundation for Promotion of Cancer Research, Grants-in-Aid for Young Scientists (B) (KAKENHI Grant Number 21791174 and 23791401) from the Ministry of Education, Culture, Sports, Science and Technology of Japan, Terumo Life Science Foundation, and Mochida Memorial Foundation for Medical and Pharmaceutical Research.

REFERENCES

(1) Coleman, R. E. (1997) Skeletal complications of malignancy. *Cancer 80*, 1588−94.

(2) Mundy, G. R. (1997) Mechanisms of bone metastasis. *Cancer 80*, 1546−56.

(3) Wong, K. K., and Piert, M. (2013) Dynamic bone imaging with ^{99m}Tc-labeled diphosphonates and ^{18}F-NaF: mechanisms and applications. *J. Nucl. Med. 54*, 590−9.

(4) Zhernosekov, K. P., Filosofov, D. V., Baum, R. P., Aschoff, P., Bihl, H., Razbash, A. A., Jahn, M., Jennewein, M., and Rosch, F. (2007) Processing of generator-produced ^{68}Ga for medical application. *J. Nucl. Med. 48*, 1741−8.

(5) Ogawa, K., Takai, K., Kanbara, H., Kiwada, T., Kitamura, Y., Shiba, K., and Odani, A. (2011) Preparation and evaluation of a radiogallium complex-conjugated bisphosphonate as a bone scintigraphy agent. *Nucl. Med. Biol. 38*, 631−6.

(6) Suzuki, K., Satake, M., Suwada, J., Oshikiri, S., Ashino, H., Dozono, H., Hino, A., Kasahara, H., and Minamizawa, T. (2011) Synthesis and evaluation of a novel ^{68}Ga-chelate-conjugated bisphosphonate as a bone-seeking agent for PET imaging. *Nucl. Med. Biol. 38*, 1011−8.

(7) Meckel, M., Fellner, M., Thieme, N., Bergmann, R., Kubicek, V., and Rosch, F. (2013) In vivo comparison of DOTA based ^{68}Ga-labelled bisphosphonates for bone imaging in non-tumour models. *Nucl. Med. Biol. 40*, 823−30.

(8) Ogawa, K., Ishizaki, A., Takai, K., Kitamura, Y., Kiwada, T., Shiba, K., and Odani, A. (2013) Development of novel radiogallium-labeled bone imaging agents using oligo-aspartic acid peptides as carriers. *PLoS One 8*, No. e84335.

(9) Schottelius, M., Laufer, B., Kessler, H., and Wester, H. J. (2009) Ligands for mapping $\alpha_v\beta_3$-integrin expression in vivo. *Acc. Chem. Res. 42*, 969−80.

(10) Niu, G., and Chen, X. (2011) Why integrin as a primary target for imaging and therapy. *Theranostics 1*, 30−47.

(11) Brooks, P. C., Clark, R. A., and Cheresh, D. A. (1994) Requirement of vascular integrin $\alpha_v\beta_3$ for angiogenesis. *Science 264*, 569−71.

(12) Brooks, P. C., Montgomery, A. M., Rosenfeld, M., Reisfeld, R. A., Hu, T., Klier, G., and Cheresh, D. A. (1994) Integrin $\alpha_v\beta_3$ antagonists promote tumor regression by inducing apoptosis of angiogenic blood vessels. *Cell 79*, 1157−64.

(13) Haubner, R., Wester, H. J., Reuning, U., Senekowitsch-Schmidtke, R., Diefenbach, B., Kessler, H., Stocklin, G., and Schwaiger, M. (1999) Radiolabeled $\alpha_v\beta_3$ integrin antagonists: A new class of tracers for tumor targeting. *J. Nucl. Med. 40*, 1061−71.

(14) Danhier, F., Le Breton, A., and Preat, V. (2012) RGD-based strategies to target $\alpha_v\beta_3$ integrin in cancer therapy and diagnosis. *Mol. Pharmaceutics 9*, 2961−73.

(15) Haubner, R., Maschauer, S., and Prante, O. (2014) PET radiopharmaceuticals for imaging integrin expression: tracers in clinical studies and recent developments. *Biomed Res. Int. 2014*, No. 871609.

(16) Gaertner, F. C., Kessler, H., Wester, H. J., Schwaiger, M., and Beer, A. J. (2012) Radiolabelled RGD peptides for imaging and therapy. *Eur. J. Nucl. Med. Mol. Imaging 39* (Suppl 1), S126−38.

(17) Yanagi, M., Uehara, T., Uchida, Y., Kiyota, S., Kinoshita, M., Higaki, Y., Akizawa, H., Hanaoka, H., and Arano, Y. (2013) Chemical design of ^{99m}Tc-labeled probes for targeting osteogenic bone region. *Bioconjugate Chem. 24*, 1248−55.

(18) Kasugai, S., Fujisawa, R., Waki, Y., Miyamoto, K., and Ohya, K. (2000) Selective drug delivery system to bone: Small peptide $(Asp)_6$ conjugation. *J. Bone Miner. Res. 15*, 936−43.

(19) Ishizaki, J., Waki, Y., Takahashi-Nishioka, T., Yokogawa, K., and Miyamoto, K. (2009) Selective drug delivery to bone using acidic oligopeptides. *J. Bone Miner. Metab. 27*, 1−8.

(20) Galasko, C. S. (1980) Mechanism of uptake of bone imaging isotopes by skeletal metastases. *Clin Nucl. Med. 5*, 565−8.

(21) Garcia, J. R., Simo, M., Perez, G., Soler, M., Lopez, S., Setoain, X., and Lomena, F. (2003) ^{99m}Tc-MDP bone scintigraphy and ^{18}F-FDG positron emission tomography in lung and prostate cancer patients: Different affinity between lytic and sclerotic bone metastases. *Eur. J. Nucl. Med. Mol. Imaging 30*, 1714.

(22) Wadas, T. J., Deng, H., Sprague, J. E., Zheleznyak, A., Weilbaecher, K. N., and Anderson, C. J. (2009) Targeting the $\alpha_v\beta_3$ integrin for small-animal PET/CT of osteolytic bone metastases. *J. Nucl. Med. 50*, 1873−80.

(23) Bakewell, S. J., Nestor, P., Prasad, S., Tomasson, M. H., Dowland, N., Mehrotra, M., Scarborough, R., Kanter, J., Abe, K.,

DOI: 10.1021/acs.bioconjchem.5b00186
Bioconjugate Chem. 2015, 26, 1561−1570

Phillips, D., et al. (2003) Platelet and osteoclast β_3 integrins are critical for bone metastasis. *Proc. Natl. Acad. Sci. U. S. A. 100*, 14205−10.
(24) Horton, M. A., Dorey, E. L., Nesbitt, S. A., Samanen, J., Ali, F. E., Stadel, J. M., Nichols, A., Greig, R., and Helfrich, M. H. (1993) Modulation of vitronectin receptor-mediated osteoclast adhesion by Arg-Gly-Asp peptide analogs: a structure-function analysis. *J. Bone Miner. Res. 8*, 239−47.
(25) Zheleznyak, A., Wadas, T. J., Sherman, C. D., Wilson, J. M., Kostenuik, P. J., Weilbaecher, K. N., and Anderson, C. J. (2012) Integrin $\alpha_v\beta_3$ as a PET imaging biomarker for osteoclast number in mouse models of negative and positive osteoclast regulation. *Mol. Imaging Biol. 14*, 500−8.
(26) Miao, W., Zheng, S., Dai, H., Wang, F., Jin, X., Zhu, Z., and Jia, B. (2014) Comparison of ^{99m}Tc-3PRGD2 integrin receptor imaging with ^{99m}Tc-MDP bone scan in diagnosis of bone metastasis in patients with lung cancer: A multicenter study. *PLoS One 9*, No. e111221.
(27) Israel, I., Richter, D., Stritzker, J., van Ooschot, M., Donat, U., Buck, A. K., and Samnick, S. (2014) PET imaging with [^{68}Ga]NOTA-RGD for prostate cancer: a comparative study with [^{18}F]-fluorodeoxyglucose and [^{18}F]fluoroethylcholine. *Curr. Cancer Drug Targets 14*, 371−9.
(28) Trajkovic-Arsic, M., Mohajerani, P., Sarantopoulos, A., Kalideris, E., Steiger, K., Esposito, I., Ma, X., Themelis, G., Burton, N., Michalski, C. W., et al. (2014) Multimodal molecular imaging of integrin $\alpha_v\beta_3$ for in vivo detection of pancreatic cancer. *J. Nucl. Med. 55*, 446−51.
(29) Liu, Z., and Wang, F. (2013) Development of RGD-based radiotracers for tumor imaging and therapy: Translating from bench to bedside. *Curr. Mol. Med. 13*, 1487−505.
(30) Chakraborty, S., Shi, J., Kim, Y. S., Zhou, Y., Jia, B., Wang, F., and Liu, S. (2010) Evaluation of ^{111}In-labeled cyclic RGD peptides: tetrameric not tetravalent. *Bioconjugate Chem. 21*, 969−78.
(31) Bozon-Petitprin, A., Bacot, S., Gauchez, A. S., Ahmadi, M., Bourre, J. C., Marti-Batlle, D., Perret, P., Broisat, A., Riou, L. M., Claron, M., et al. (2014) Targeted radionuclide therapy with RAFT-RGD radiolabelled with ^{90}Y or ^{177}Lu in a mouse model of $\alpha_v\beta_3$-expressing tumours. *Eur. J. Nucl. Med. Mol. Imaging.*, 252−63.
(32) Yoshimoto, M., Ogawa, K., Washiyama, K., Shikano, N., Mori, H., Amano, R., and Kawai, K. (2008) $\alpha_v\beta_3$ Integrin-targeting radionuclide therapy and imaging with monomeric RGD peptide. *Int. J. Cancer 123*, 709−15.
(33) Ogawa, K., and Washiyama, K. (2012) Bone target radiotracers for palliative therapy of bone metastases. *Curr. Med. Chem. 19*, 3290−300.
(34) Ogawa, K., Mukai, T., Asano, D., Kawashima, H., Kinuya, S., Shiba, K., Hashimoto, K., Mori, H., and Saji, H. (2007) Therapeutic effects of a ^{186}Re-complex-conjugated bisphosphonate for the palliation of metastatic bone pain in an animal model. *J. Nucl. Med. 48*, 122−7.
(35) Ogawa, K., Mukai, T., Arano, Y., Otaka, A., Ueda, M., Uehara, T., Magata, Y., Hashimoto, K., and Saji, H. (2006) Rhenium-186-monoaminemonoamidedithiol-conjugated bisphosphonate derivatives for bone pain palliation. *Nucl. Med. Biol. 33*, 513−20.
(36) Ogawa, K., Mukai, T., Arano, Y., Ono, M., Hanaoka, H., Ishino, S., Hashimoto, K., Nishimura, H., and Saji, H. (2005) Development of a rhenium-186-labeled MAG3-conjugated bisphosphonate for the palliation of metastatic bone pain based on the concept of bifunctional radiopharmaceuticals. *Bioconjugate Chem. 16*, 751−7.
(37) Ogawa, K., Kawashima, H., Shiba, K., Washiyama, K., Yoshimoto, M., Kiyono, Y., Ueda, M., Mori, H., and Saji, H. (2009) Development of [^{90}Y]DOTA-conjugated bisphosphonate for treatment of painful bone metastases. *Nucl. Med. Biol. 36*, 129−35.
(38) Notni, J., Pohle, K., and Wester, H. J. (2012) Comparative gallium-68 labeling of TRAP-, NOTA-, and DOTA-peptides: practical consequences for the future of gallium-68-PET. *EJNMMI Res. 2*, 28.
(39) Dijkgraaf, I., Kruijtzer, J. A., Liu, S., Soede, A. C., Oyen, W. J., Corstens, F. H., Liskamp, R. M., and Boerman, O. C. (2007) Improved targeting of the $\alpha_v\beta_3$ integrin by multimerisation of RGD peptides. *Eur. J. Nucl. Med. Mol. Imaging 34*, 267−73.
(40) Ogawa, K., Mukai, T., Inoue, Y., Ono, M., and Saji, H. (2006) Development of a novel ^{99m}Tc-chelate-conjugated bisphosphonate with high affinity for bone as a bone scintigraphic agent. *J. Nucl. Med. 47*, 2042−7.
(41) Ogawa, K., Mukai, T., Kawai, K., Takamura, N., Hanaoka, H., Hashimoto, K., Shiba, K., Mori, H., and Saji, H. (2009) Usefulness of competitive inhibitors of protein binding for improving the pharmacokinetics of ^{186}Re-MAG3-conjugated bisphosphonate (^{186}Re-MAG3-HBP), an agent for treatment of painful bone metastases. *Eur. J. Nucl. Med. Mol. Imaging 36*, 115−21.

DOI: 10.1021/acs.bioconjchem.5b00186
Bioconjugate Chem. 2015, 26, 1561−1570